AQUATIC ECOLOGY

10.1126/sciadv.1501660

Long-term dynamics of adaptive evolution in a globally important phytoplankton species to ocean acidification

Lothar Schlüter,[1] Kai T. Lohbeck,[1†] Joachim P. Gröger,[2] Ulf Riebesell,[3] Thorsten B. H. Reusch[1]*

Marine phytoplankton may adapt to ocean change, such as acidification or warming, because of their large population sizes and short generation times. Long-term adaptation to novel environments is a dynamic process, and phenotypic change can take place thousands of generations after exposure to novel conditions. We conducted a long-term evolution experiment (4 years = 2100 generations), starting with a single clone of the abundant and widespread coccolithophore *Emiliania huxleyi* exposed to three different CO_2 levels simulating ocean acidification (OA). Growth rates as a proxy for Darwinian fitness increased only moderately under both levels of OA [+3.4% and +4.8%, respectively, at 1100 and 2200 µatm partial pressure of CO_2 (Pco_2)] relative to control treatments (ambient CO_2, 400 µatm). Long-term adaptation to OA was complex, and initial phenotypic responses of ecologically important traits were later reverted. The biogeochemically important trait of calcification, in particular, that had initially been restored within the first year of evolution was later reduced to levels lower than the performance of nonadapted populations under OA. Calcification was not constitutively lost but returned to control treatment levels when high CO_2–adapted isolates were transferred back to present-day control CO_2 conditions. Selection under elevated CO_2 exacerbated a general decrease of cell sizes under long-term laboratory evolution. Our results show that phytoplankton may evolve complex phenotypic plasticity that can affect biogeochemically important traits, such as calcification. Adaptive evolution may play out over longer time scales (>1 year) in an unforeseen way under future ocean conditions that cannot be predicted from initial adaptation responses.

INTRODUCTION

About half of global primary production is contributed by marine phytoplankton (*1*), microscopic algae that form the base of marine food webs and play a major role in global biogeochemical cycles. They turn inorganic carbon and minerals into particulate organic matter that may eventually be transported into the deep ocean through sedimentation, a process known as the biological carbon pump (*2*). Coccolithophores, one of the important phytoplankton groups in contemporary oceans, are important contributors to the ballasting of organic particles (*3*). This is because their cells are covered by minute calcite platelets, coccoliths, which have a much higher density than seawater. Like many marine calcifying organisms, coccolithophores suffer from ocean acidification (OA) (*4*), resulting from the dissolution of excess anthropogenic CO_2 in ocean waters (*5*). A wealth of short-term experiments where coccolithophores were exposed to OA conditions revealed an immediate response pattern of decreased calcification and growth rates (*6*, *7*). Recent evolution experiments demonstrated, in line with evolutionary theory and results in model microbes, adaptation to OA and warming in the globally important coccolithophore *Emiliania huxleyi*, both through genotypic selection in multiclone assays and through de novo mutations (*8*, *9*). The above studies ran for approximately 1 year (≈500 asexual generations). From evolutionary model species, such as *Escherichia coli* and yeast, it is well known that adaptive evolution is a dynamic long-term process even in the simplest experiments, designed with a single clone (or genotype) as the starting "population." For example, adaptation to novel conditions through selective sweeps may be delayed by clonal interference (*10*, *11*), adaptive improvements may be sudden and stepwise when mutations are rare (*12*), and consecutive beneficial mutations may depend on one another, introducing lineage-specific historical contingency (*13*). Hence, further phenotypic changes can occur over several thousand generations. For example, in *E. coli*, an adaptation to citrate utilization arose 31,500 generations after initial exposure to glucose minimal medium that was citrate-enriched (*13*). A recent 15-year time series reports evidence for adaptive changes of natural phytoplankton communities to yearly variation in environmental conditions (temperature and irradiance) (*14*).

Here, we evolved replicate populations derived from a single clone of *E. huxleyi* for 2100 asexual generations (4 years) to ambient [400 µatm partial pressure of CO_2 (Pco_2)] and two elevated Pco_2, simulating different levels of OA (*5*). We chose a medium level projected for the end of this century for a worst-case CO_2 emission scenario (1100 µatm) (*15*) and a high proof-of-principle treatment (2200 µatm Pco_2). Already now, these levels are temporarily found in coastal waters under upwelling of oxygen-deficient waters (*16*). Upon initial findings of a partial restoration of calcification in *E. huxleyi* (*8*), we were particularly interested in how calcification played out in subsequent years. Another important question was whether adaptive evolution would lead to complete restoration of algal performance and fitness under OA compared to nonadapted controls when both were assayed under OA conditions.

[1]Evolutionary Ecology of Marine Fishes, GEOMAR Helmholtz Centre for Ocean Research Kiel, Düsternbrooker Weg 20, 24105 Kiel, Germany. [2]Living Marine Resources Research Unit, Thünen-Institute of Sea Fisheries, Palmaille 9, 22767 Hamburg, Germany. [3]Biological Oceanography, GEOMAR Helmholtz Centre for Ocean Research Kiel, Düsternbrooker Weg 20, 24105 Kiel, Germany.
*Corresponding author. Email: treusch@geomar.de
†Present address: Department of Marine Sciences, University of Gothenburg, 41319 Gothenburg, Sweden.

RESULTS

Over 2100 asexual generations, mean exponential growth rates in all treatments increased with time [daily growth rates (μ) per generation: ambient CO_2: 6.56×10^{-5}; medium CO_2: 4.33×10^{-5}; high CO_2: 7.60×10^{-5}; autoregressive-moving average models with exogenous variables (ARMAX) model with significant autocorrelation terms, all trends $P < 0.001$], with no detectable difference between OA treatments (Fig. 1A). In contrast, cell diameter decreased over time in all treatments, again with no difference among treatment levels (ARMAX model, all trends $P < 0.001$; Fig. 1B). Thus, cells had between 12 and 22% less volume at the end of year 4 compared to the starting genotype. These background changes, owing to the general selection regime in the laboratory, need to be taken into account when interpreting the adaptive responses because of simulated OA.

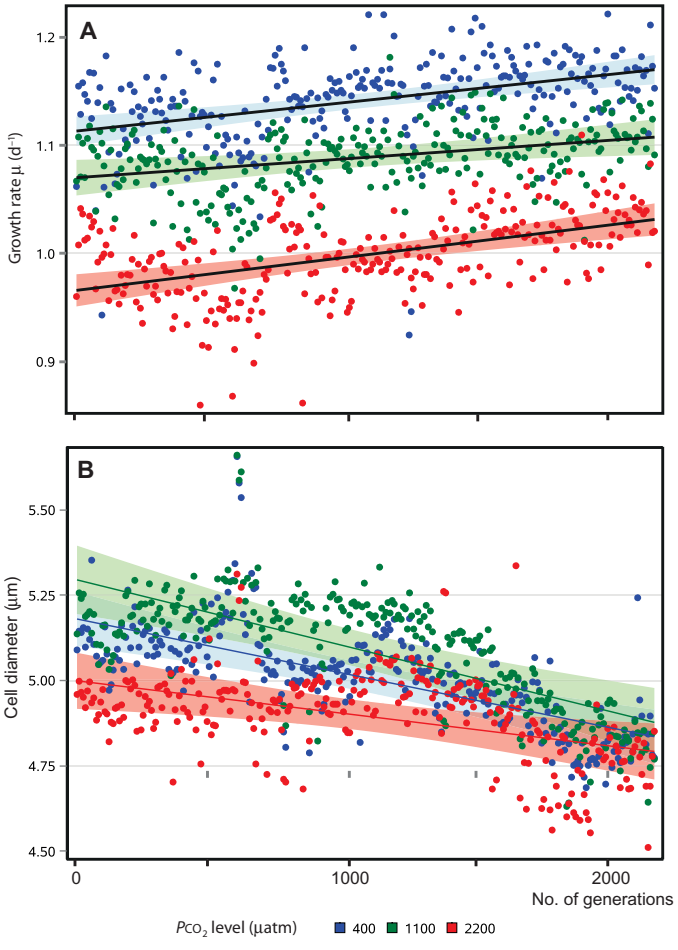

Fig. 1. Long-term phenotypic changes in replicated batch cultures of *E. huxleyi* under control and OA conditions. (A and **B**) Time course of specific daily growth rate (A) and cell diameter (B) over 4 years of selection to three different P_{CO_2} levels, simulating OA. Growth rates and cell sizes were calculated every 5 days upon transfer of batch cultures. All lines reveal highly significant slopes that are not significantly different among CO_2 treatments. Because we were not specifically interested in detecting a response level difference but differences in the time trends (that is, slopes), and as temporal variables are usually autocorrelated, the trend lines were not estimated on the basis of simple regression but using a series of ARMAX models (including transfer functions; for details, see Materials and Methods).

To assess evolutionary responses to elevated CO_2 and to control for general laboratory adaptation, we measured growth rates of medium CO_2– and high CO_2–adapted populations in the respective elevated CO_2 environment through reciprocal assay experiments relative to control populations that, at the same time, had evolved under ambient CO_2 conditions (*17*). In all assay experiments, populations were acclimated for at least one full batch cycle (seven to eight asexual generations) to their novel condition. Assay experiments were conducted at five time points (approximately 500, 1000, 1200, 1600, and 2100 asexual generations) and also included a test of the correlated response, the back-exposure of populations evolved under elevated CO_2 to ambient conditions (fig. S1).

We focus here on the time course of the adaptive response (Fig. 2), which is given by the difference between control populations (always depicted as a black thin line) relative to populations that were allowed to long-term adapt to OA, both tested under OA conditions. In all assay experiments, CO_2-selected population grew faster than nonadapted ones when assayed under both medium and high CO_2 [medium CO_2 selection: $F_{1,8} = 43.92$, $P = 0.0002$, repeated-measures analysis of variance (rmANOVA); high CO_2 selection: $F_{1,8} = 53.72$, $P < 0.0001$, rmANOVA; Fig. 2, A and B]. Growth rate adaptation increased over time under medium CO_2 selection (time × selection: $F_{4,32} = 2.941$, $P = 0.035$, rmANOVA). Under high CO_2 selection, the adaptation effect was continually present and did not increase further, nor was there a significant fluctuation of the adaptive response [time × selection: $F_{4,32} = 1.991$, $P =$ not significant (ns), rmANOVA]. Except for the first assay experiment after approximately 500 generations, medium CO_2– and high CO_2–selected populations grew slower compared to controls under ambient P_{CO_2} (fig. S1A), thus revealing a cost to adaptation.

Next, we focused on ecologically important cell traits that were not directly subjected to selection, such as cell sizes and elemental quotas, but may be correlated with asexual fitness. For cell size, the phenotype changed in the course of the 4-year experiment. Although medium CO_2– and high CO_2–selected cells were initially larger, they became smaller after 1400 generations relative to control populations (time × CO_2: medium CO_2 selection: $F_{4,32} = 11.44$, $P < 0.0001$, rmANOVA; time × high CO_2 selection: $F_{4,32} = 10.89$, $P < 0.0001$, rmANOVA; Fig. 2, C and D), although the main effect CO_2 selection was not significant (medium: $F_{1,8} = 0.762$, $P =$ ns, rmANOVA; high: $F_{1,8} = 0.593$, $P =$ ns, rmANOVA). Note that cell size changes associated with adaptation to elevated CO_2 are superimposed by a general trend toward smaller cells in all treatments (Fig. 1B).

The particulate organic carbon (POC) content of the cells decreased over time in both selection treatments as a consequence of elevated CO_2. Compared to short-term exposed controls, we observed a decrease of POC content under both medium and high CO_2 selection (medium CO_2 selection: $F_{1,7} = 18.13$, $P = 0.0038$, rmANOVA; high CO_2 selection: $F_{1,6} = 17.45$, $P = 0.0058$, rmANOVA; Fig. 2, E and F), with the interaction with time being nonsignificant in both cases. Except for a nonsignificant increase at 1000 generations, the general decrease in POC is also apparent for all three selection treatments under ambient CO_2 (correlated response; fig. S1C). Hence, the general laboratory conditions may have selected for cells with less organic carbon content. Because there was a 12 to 22% general decrease in cell volume across treatments, we also standardized cell quota by cell volume. The general picture remained the same, especially in the high CO_2 selection treatment, namely, we found an additional decrease in the treatments long-term adapted to elevated CO_2 (medium CO_2 selection: $F_{1,7} = 6.47$, $P = 0.0384$, rmANOVA; high CO_2 selection: $F_{1,6} = 12.42$, $P = 0.0124$, rmANOVA; fig. S2, A and B).

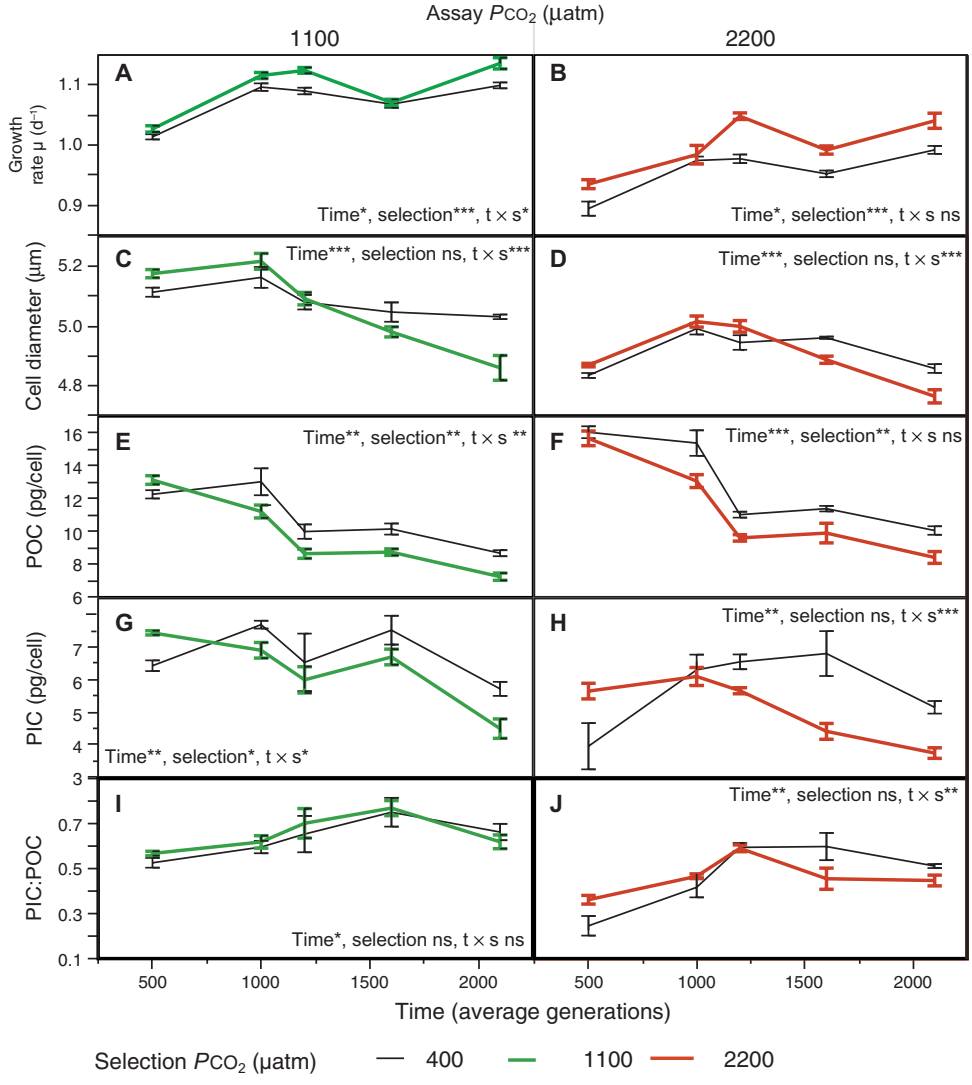

Fig. 2. Adaptive response of *E. huxleyi* to selection under three P_{CO_2} levels simulating OA. Adaptive response over 4 years measured during assay experiments at five time points (*x* axis, average generations of all three CO_2 treatments), always comparing medium CO_2–adapted (left) and high CO_2–adapted (right) versus nonadapted populations of *E. huxleyi* in three different CO_2 environments, when assayed under elevated CO_2 (mean ± SD, $n = 5$). (**A** and **B**) Exponential growth rate. (**C** and **D**) Cell diameter. (**E** and **F**) POC per cell. (**G** and **H**) PIC per cell. (**I** and **J**) Ratio of PIC/POC. Significant results of main and interaction effects are depicted with asterisks (*$0.05 \geq P > 0.01$, **$0.01 \geq P > 0.001$, ***$P < 0.001$). Complete rmANOVA results are given in table S1. The correlated response, that is, the performance of all high CO_2 selection treatments under ambient CO_2, is presented in fig. S1.

We were particularly interested in how cell quotas in particulate inorganic carbon (PIC) would change throughout the selection experiment. We expected that, given sufficient time, the observed partial restoration of PIC cell quotas under OA compared to controls after 500 generations (*8*) would be completely restored in both medium and high CO_2 selection treatments. Contrary to expectations, PIC cell quotas markedly decreased after generation 1000 to be lower in populations adapted to high CO_2 than in nonadapted controls when subjected to OA conditions (time × CO_2: medium CO_2 selection: $F_{4,28} = 4.85$, $P = 0.0042$, rmANOVA; high CO_2 selection: $F_{4,24} = 6.79$, $P = 0.0008$, rmANOVA; Fig. 2, G and H). In response to medium and high CO_2 selection, CO_2-adapted populations displayed 21 and 22% lower PIC, respectively, compared to the physiological decline of PIC in the control populations under medium and high CO_2 (all at 2100 generations; Fig. 2, G and H). This pattern also remained after we standardized PIC content on cell volume to compensate for the general decrease in cell size over time (time × CO_2: medium CO_2 selection: $F_{4,28} = 3.95$, $P = 0.0115$, rmANOVA; high CO_2 selection: $F_{4,24} = 5.58$, $P = 0.0025$, rmANOVA; fig. S2, C and D). In terms of PIC/POC ratio, we found an interaction of time and CO_2 selection in the high, but not in response to the medium, CO_2 selection (time × CO_2: medium: $F_{4,28} = 0.3378$, $P =$ ns, rmANOVA; high: $F_{4,24} = 6.36$, $P = 0.0012$, rmANOVA; Fig. 2, I and J).

For the final assay experiment at generation 2100, we plotted population-wise reaction norms for important parameters under ambient and elevated CO_2 levels to address the evolution of plasticity in traits other than fitness itself that accompanied adaptation (details of statistical analysis are in table S2; Fig. 3, A and B). After 4 years, corresponding to ~2100 asexual generations, we observed an increase of

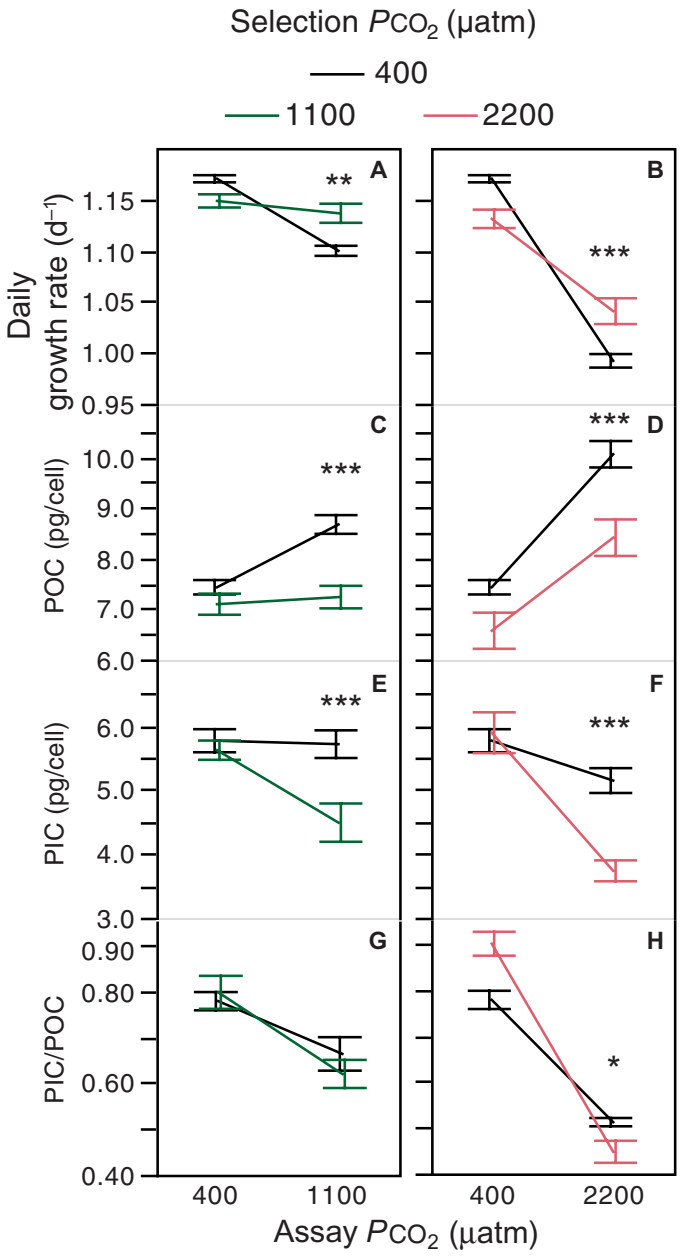

Fig. 3. End-point reaction norms of *E. huxleyi* populations selected under ambient and high CO_2 conditions as a function of the assay condition. (**A** to **H**) Daily growth rate (A and B), POC (C and D), PIC (E and F), and PIC/POC ratio (G and H) after 2100 generations of evolution (~4 years). Given are means (±1 SD, n = 5). Significant results of planned contrasts are given only for the adaptation response (that is, under elevated CO_2) and are indicated by asterisks (*0.05 ≥ P > 0.01, **0.01 ≥ P > 0.001, ***P < 0.001).

asexual fitness in both selection treatments, resulting in 3.4 and 4.8% increase [calculated according to Lenski *et al.* (*18*)] under medium and high CO_2, respectively, compared to control populations. Except for generation 500, adaptation to OA at all later time points was accompanied with "classical" costs of adaptation in both medium and high CO_2 when back-exposed at ambient CO_2 (interaction selection × assay CO_2: all P < 0.001, two-way ANOVA at each time point; fig. S1, A and B).

The reaction norms of the POC quota of cells after CO_2 selection revealed a strong "overshooting" response of POC cell quota of non-adapted populations under medium (+20% POC; Fig. 3C) and high CO_2 assay conditions (+19%; Fig. 3D) compared to high CO_2–adapted ones. However, slopes of the reaction norms in response to assay CO_2 were only significantly different among ambient CO_2–selected versus medium CO_2–selected populations (interaction selection × assay CO_2: P = 0.011, two-way ANOVA; Fig. 3, C and D). Also, medium CO_2–adapted populations restored their POC quotas under high CO_2 to levels observed in controls under ambient CO_2 (planned contrast, P = ns; Fig. 3C), whereas there was still 11% more POC per cell for the high CO_2–selected replicates tested under high CO_2 compared to the ambient control (planned contrast, P = 0.0368; Fig. 3D).

For calcification (assessed as PIC cell quota), populations selected for 4 years to OA showed markedly different reaction norms and, hence, evolved a different pattern of phenotypic plasticity (interaction selection × assay CO_2: P = 0.022 and 0.0033 for medium and high selection, respectively). Despite the loss of calcification under OA assay conditions, CO_2-selected populations increased their PIC quota when transferred back into ambient CO_2 (+25% for medium CO_2 selection, Fig. 3E; +58% for high selection, Fig. 3F; planned contrast, both P < 0.001), which was then indistinguishable from control populations under ambient CO_2. As a result of both changes in POC and PIC cell quota reaction norms, the PIC/POC ratio changed, which, in turn, determines the specific mass and, hence, the contribution to enhanced sinking velocity of organic matter by an individual coccolithophorid cell (Fig. 3, G and H). Here, for the high CO_2–selected populations only, the PIC/POC ratio was significantly reduced after long-term adaptation under high CO_2 while overcompensated upon reexposure to ambient CO_2 (Fig. 3H).

DISCUSSION

Our experiment is the first to describe long-term adaptation for a few thousand generations in any marine microbial species, including phytoplankton (*19*). Before the experiment, we expected the previously identified adaptation response in growth rates after 1 year (*8*) between treatments subjected to long-term OA versus controls to increase. However, the adaptation response did only increase marginally with time for the low, but not the high, CO_2 levels, suggesting either some fundamental constraints to adaptation to OA or that waiting times for required rare mutations were exceedingly long. This was different for important correlated traits, such as elemental cell quotas, in particular, the inorganic and organic carbon content of individual cells, where responses partly reverted between years 1 and 4. Hence, even 1 year of evolutionary change reported earlier (*8*) may only cover a transient response in these traits when compared to longer time intervals. These complex long-term dynamics have also been found in selection experiments with model microbes (*11*, *13*, *20*). Whereas these species lack an immediate ecological or biogeochemical significance, our results have implications for marine primary production and carbon sequestration, given the important role of phytoplankton in general and that of *E. huxleyi* as the world's most abundant calcifying phytoplankton species in particular (*21*). Specifically, we show that long-term evolution can exacerbate the immediate physiological decline in calcification, which is assessed here as PIC cell quotas. This reverted the initial notions after 1 year of adaptation to OA, which revealed partial rescue

of calcification (*8*). The reverse response under OA adaptation observed here would decrease the ballasting effect of an individual coccolithophorid cell adapted to OA. If extrapolated to the ocean, this, in turn, may have negative consequences for the ocean's biological carbon pump, along with the general abundance of coccolithophores in a phytoplankton community (*3*).

Mutational dynamics in an asexual diploid

How these changes in the adaptive dynamics came about is currently elusive. It may be that genotypes that calcified less under high CO_2 levels, and thus were already "plastic" with respect to producing calcite plates, arose within the first year of experimental duration. However, they only rose to (near) fixation during the subsequent years because of competition with other genotypes carrying other favorable mutations owing to clonal interference (*22*). Recent experiments in a yeast model species under asexual reproduction and diploidy have revealed rampant genetic hitchhiking and clonal competition during the course of simple evolution experiments (*11*), leading to unpredictable time lags and nonsynchronous adaptation processes. Alternatively, mutations affecting the regulation of calcification may have a smaller mutational target and are thus much less common, meaning that the waiting time to such mutations is longer than 1 year.

To assess the contributions of initially rare genotypes and to follow their dynamics, one would have to take many subreplicates during the run time of the experiment, which was prohibited by the large logistical effort to grow *E. huxleyi* in appreciable population sizes in the laboratory. Growth rate is the parameter we selected for and directly reflects the Darwinian fitness in our asexually reproducing batch populations (*18*).

Dynamics of correlated cell traits

How other traits respond to CO_2 selection depends upon the genetic architecture (for example, genetic correlations) and on the contribution of any particular trait to fitness (that is, its fitness function). Parameters such as cell size are probably correlated with cell division and thus exponential growth rates of the batch cultures to a certain extent (*23*). In our experiment, the decrease in cell volume of up to 22% (Fig. 1B) observed in all treatments was mainly driven by our selection regime of sequential batch cultures, favoring maximal exponential growth rates and thus resulting in smaller cells. When subtracting the decline in cell volume attributable to selection for fast growth, assay experiments revealed that there is still an additional decrease of POC, which is caused by selection to increased CO_2 (cf. an absolute difference of 1.6 and 1.8 pg POC per cell among medium and high selected treatments and controls in Fig. 2, E and F, during both final time points). These findings contrast the adaptive responses we observed after 500 generations (*8*) of nearly similar POC cell quotas. At this point, we can only speculate that prolonged selection under nutrient-replete culture conditions may have favored an altered cellular carbon storage strategy, resulting in smaller cells containing less organic carbon compared to the ancestral population. This is particularly interesting in the light of short-term physiological responses to OA, which are characterized by an increase in organic storage compounds, including lipids and glucans (*24*). More detailed physiological assessments along the time course of experimental evolution are clearly warranted to dissect the cellular mechanisms, costs, and constraints determining the observed phenotypic responses. However, note that the specific time course of adaptation, correlated responses, and trait evolution may be contingent upon the particular genotype (clone #62) that was chosen to initiate the experiment (*25*). Even if the genetic starting material is completely identical, historical chance events may produce idiosyncratic outcomes of evolution when "rewinding the evolutionary tape" (*13*). We can only speculate whether or not other starting genotypes would have evolved a similar plastic response. What is clear, is that the sensitivity to OA in terms of calcification declines already varies among existing genotypes (*26*).

Possible mechanisms driving PIC changes

How coccolith formation and, hence, the PIC cell quota are linked to fitness still remains elusive (*27*). The biogenic precipitation of calcium carbonate is an energy-demanding process, with energetic costs expected to increase under elevated CO_2 (*28*). When initiating the long-term selection experiment with *E. huxleyi*, we expected a reduction in calcification as one adaptation mechanism to OA. This was based on the assumption that a selective pressure to maintain coccolith formation is absent in our enemy-free batch culture system. The initial partial restoration of PIC quotas and calcification rates during the first year of experimental evolution (*8*) refuted those ideas. However, the subsequent evolutionary dynamics reported here is now consistent with these initial expectations after about generation 1000. The ability to calcify was not constitutively lost in high CO_2–adapted populations, but we observed the evolution of a flexible response, that is, phenotypic plasticity. Although we found a complete restoration of PIC quotas under ambient CO_2, elevated CO_2 selection resulted in a further decrease of PIC, and this decrease was significantly lower than the immediate physiological response of control populations to OA.

The evolution of phenotypic plasticity

Phenotypic plasticity describes how the same genotype gives rise to different phenotypes in response to different environments (*29*). One important aspect of studying phenotypic plasticity is to investigate how different genotypes of a particular phytoplankton species respond to higher CO_2 levels. To address how phytoplankton growth and photosynthesis rates are affected by higher dissolved inorganic carbon (DIC) availability associated with increasing CO_2 is important to predict primary productivity in future ocean conditions, particularly in noncalcifying species (*30*). Coccolithophores only benefit from increased DIC availability at relatively low levels (*E. huxleyi* up to 600 µatm P_{CO_2}) (*31*). If the net CO_2 effect on growth rates is negative under higher OA levels (beyond 1000 µatm P_{CO_2}), as in *E. huxleyi*, phenotypic buffering may extend the range of tolerances and keep organismal function even under OA (*32*). Here, we found that an energetically costly trait, namely, biogenic calcification (*21*, *28*), is reduced because of long-term selection under high CO_2 conditions, whereas it is almost unchanged when high CO_2–adapted populations are back-exposed to the ancestral condition (ambient CO_2 concentration). Thus, the high CO_2–adapted replicates have evolved a pattern of phenotypic plasticity in the high CO_2 environment (*33*), which is consistent with an adaptive reduction of calcification when it is costly. They now reveal two distinct phenotypes—one with reduced and one with "normal" PIC cell quotas—as a function of the assay CO_2 environment (=correlated response). In a selection experiment with increased CO_2 in the freshwater alga *Chlamydomonas*, conditionally deleterious mutations were believed to have accumulated in the high CO_2 selection lines, leading to lower growth when reexposed to ambient CO_2 because of deterioration of carbon-concentrating mechanisms (CCMs) (*34*). Hypothetically, such a loss of CCM may

also be the mechanism leading to costs of CO_2 adaptation in the medium CO_2– and high CO_2–selected replicates past generation 1000. In contrast, during the first 500 generations, we have to invoke the accumulation of gain-of-function mutations that were only visible when comparing control to adapted populations in the novel environment. They probably involved regulatory regions because the phenotypic effects were reversible and only visible in the high CO_2 assay environment.

The process of calcification requires tight metabolic regulation, such as pH regulation and directed Ca^{2+} and HCO_3^- transport to the coccolith vesicle before the precipitation of calcite itself (*28*, *35*). Under OA conditions, the regulation of the cytosolic pH is compromised and decreases (*24*, *36*). Although not only critical for calcification, pH homeostasis is important for many metabolic processes. Initially, adaptation may have improved cellular pH regulation under high CO_2 conditions, and calcification may have partly been restored by passively following this adaptive regulatory response (*37*). The later decrease in calcification suggests that, beyond approximately 1000 generations, independent of putative further improvements in pH regulation (determining growth rates), calcification was also directly affected. From a cellular metabolic perspective, it seems likely that a complex process like calcification is deeply tangled with various other metabolic pathways, limiting the regulatory capacity of calcification for the sake of pH homoeostasis. We can only speculate that, at some point beyond 1000 generations under high CO_2, calcification became less tightly coupled with other essential processes and, as a consequence, gained new regulatory flexibility. This could explain the novel patterns in phenotypic plasticity we have observed after 2100 generations.

Ecological implications

Care needs to be taken when translating our results from laboratory batch cultures to the natural system. For example, we always kept our cultures in exponential phase to maintain the desired treatment levels of OA, whereas in nature, population densities in bloom situations lead to much higher competition strength. In nature, trade-offs with other important functions of calcification and coccolith production [for example, grazer or viral defense (*27*, *38*)] will most likely prohibit the evolution of phenotypic plasticity with respect to coccolith formation observed here. Also, by starting with a single genotype, we only allowed for novel mutations as driver of evolutionary adaptation, whereas genotypic selection will most likely be equally or even more important in nature (*8*, *39*).

Experimental evolution fills the gap between paleontological studies of evolutionary changes (*40*) and field time series (*14*) by directly addressing the evolutionary dynamics on a time scale of months to years. Although evolution in response to OA can often only be observed throughout a single generation in other species (*41*, *42*), phytoplankton species lend themselves to direct experimentation (*39*, *43*). However, experimental control is likely to be traded off against realism. Our data demonstrate that caution is advised even in the simplest experimental setups, as responses after 1 year of adaptation may be transient. Clearly, more complex designs are highly warranted, for example, those that compare varying versus constant selection regimes (*44*). Also, experiments including competitors, pathogens, and predators are clearly desirable to simulate adaptive evolution under more realistic conditions as one component of phytoplankton community change in a future ocean (*39*, *45*).

MATERIALS AND METHODS

The asexual populations in this experiment originated from a single cell, which is isolated in May 2009 from the coastal waters off Bergen, Norway [clone #62; (*8*)]. Populations were kept in artificial seawater [ASW; (*46*)] medium [for details, see the study by Lohbeck *et al.* (*8*)]. To achieve a total alkalinity (TA) of 2380 μmol kg^{-1}, 0.19 g of bicarbonate per kilogram of ASW was added. CO_2 levels were manipulated by aerating the ASW medium for 24 hours at 15°C under saturated humidity with CO_2-enriched air before culture flasks were inoculated. The cultures were kept under nonaxenic condition because using antibiotics would have caused problems in maintaining the cultures over several years in exponential phase.

The selection experiment was carried out in a semicontinuous batch culture system with five replicates each for ambient (400 μatm P_{CO_2}, control), medium (1100 μatm P_{CO_2}), and high (2200 μatm P_{CO_2}) under continuous rotation (0.5 per min) at 15°C at a photon flux density of 150 μmol m^{-2} s^{-1} and a 16:8-hour light/dark cycle. Serial transfer experiments, where the same number of cells are always transferred to the next batch cycle, by definition, represent a selection for (asexual) growth rate. Those genotypes with a higher growth rate will increase in frequency and can eventually prevail in the population (*17*).

CO_2 selection was initiated in May 2010 and lasted for 268 batch cycles (~4 years), corresponding to ~2100 generations of asexual reproduction. The populations were grown in Schott Duran flasks with minimal headspace in a total volume of 310 ml. Every 5 days, 10^5 cells per replicate were transferred into the next batch. Cell density and size were determined at each transfer using a Coulter Counter Z2 Particle/Size Analyzer. Daily growth rates (μ) were calculated from cell densities according to $\mu = (\ln N_d - \ln N_0)/d$, where N_0 and N_d are cell numbers at the beginning and end of the batch cycle, and d is the duration of the batch cycle in days ($d = 5$). For the assay experiments conducted after ~500, 1000, 1200, 1600, and 2100 asexual generations, treatments grown at 400 μatm control P_{CO_2} were acclimated over one full batch cycle to the respective elevated CO_2 levels and vice versa. Growth rates and additional correlated traits were then measured along with the long-term evolved treatments under medium and high CO_2 assay conditions (adaptive response). Replicates evolving at 1100 and 2200 μatm P_{CO_2}, respectively, were also back-transferred to ambient CO_2 to assess the correlated response along with control replicates. The experimental design was incomplete because, for logistical reasons, the reciprocal exposure of 1100 and 2200 μatm P_{CO_2} was omitted. Dissolved inorganic carbon was measured colorimetrically using a SOMMA autoanalyzer or an AIRICA system (MARIANDA). P_{CO_2} values before inoculation were calculated from DIC and TA using the program CO2SYS (*47*). The drawdown of TA and DIC during the batch cycles was calculated from the total particular carbon measurements at the end of the batch cycle. The average DIC drawdown ± 1 SD was about 4% with a maximum of 7%. The measured P_{CO_2} varied from the desired level (ambient: 430 ± 32 μatm; medium: 1350 ± 207 μatm; high: 2398 ± 200 μatm). During the selection phase, one replicate of the high CO_2 selection line was temporarily contaminated with low numbers of heterotrophic nanoflagellates (<1% in cell number). If excluded, none of the statistical results changed qualitatively; therefore, the analyses present the full data set.

The cultures were vacuum-filtered (<100 mbar) onto precombusted glass fiber filters (GF/F) for the quantification of total particulate carbon and POC. All filtrations were performed at the same time of the

day (~4 to 5 hours after start of light phase). POC filters were fumed with 37% HCl for 2 hours to remove inorganic carbon and then dried at 60°C for 12 hours. The measurements were performed with elemental analyzers. PIC was calculated by subtracting HCl-fumed POC from TPC values.

We estimated changes in terms of cell sizes and growth rates using autogeressive moving average model (ARMAX) with transfer functions and autocorrelation terms if appropriate, according to

$$\text{Response} = b_0 + b_1 * d_1 * t + b_2 * d_2 * t + b_3 * d_1 + \text{ARMA terms} \quad (1)$$

where d_i in {0,1} is a dummy variable [*i*th $d_1\ t_i = 1$ if observation *i* at time *t* belongs to treatment 1 and $d_1\ t_i = 0$; else, $d_2\ t_i = 1 - (d_1\ t_i)$ indicates whether ($d_2\ t_i = 1$) or not ($d_2\ t_i = 0$) the observation belongs to treatment 2]. Hypotheses of significant slopes and treatment differences were assessed using conventional *t* and *F* tests. Note that, according to Eq. 1, dynamic effects are assumed to be the same in both of the samples. This assumption is justified theoretically because of the unified experimental design and is empirically corroborated by preliminary empirical tests.

For the statistical analysis of the reciprocal assay experiments, the data set was subdivided, for each level of elevated CO_2, into two parts to avoid singularities. In order to avoid data interdependencies of the same replicates measured at two different assay conditions and to accurately represent the distinct hypotheses, we analyzed the adaptive and correlated responses separately. For each subset, an rmANOVA including a sphericity test for the within-subject terms was conducted using JMP v. 9.0 (StatSoft Inc.). Subsequent post hoc contrasts were performed if appropriate. The final assay experiment was subjected to two-way ANOVA, with subsequent planned contrasts, separately for each CO_2 treatment. We checked for homogeneity of variances and normal distribution and found no major violation to the test assumptions.

SUPPLEMENTARY MATERIALS

Supplementary material for this article is available at http://advances.sciencemag.org/cgi/content/full/2/7/e1501660/DC1

fig. S1. Correlated response of *E. huxleyi* adapted to elevated CO_2 levels.

fig. S2. Adaptive response of *E. huxleyi*: PIC and POC cell quotas standardized to cell volume.

table S1. Statistical analysis (rmANOVA) of the adaptive response of *E. huxleyi* (cf. Fig. 2 and fig. S2).

table S2. Statistical analysis (two-way ANOVA) of the reciprocal assay in *E. huxleyi* at the end of the experiment (cf. Fig. 3).

REFERENCES AND NOTES

1. C. B. Field, M. J. Behrenfeld, J. T. Randerson, P. Falkowski, Primary production of the biosphere: Integrating terrestrial and oceanic components. *Science* **281**, 237–240 (1998).
2. P. G. Falkowski, T. Fenchel, E. F. Delong, The microbial engines that drive Earth's biogeochemical cycles. *Science* **320**, 1034–1039 (2008).
3. R. A. Armstrong, C. Lee, J. I. Hedges, S. Honjo, S. G. Wakeham, A new, mechanistic model for organic carbon fluxes in the ocean based on the quantitative association of POC with ballast minerals. *Deep-Sea Res. Pt. II* **49**, 219–236 (2001).
4. K. J. Kroeker, R. L. Kordas, R. N. Crim, G. G. Singh, Meta-analysis reveals negative yet variable effects of ocean acidification on marine organisms. *Ecol. Lett.* **13**, 1419–1434 (2010).
5. K. Caldeira, M. E. Wickett, Oceanography: Anthropogenic carbon and ocean pH. *Nature* **425**, 365 (2003).
6. J. Meyer, U. Riebesell, Reviews and syntheses: Responses of coccolithophores to ocean acidification: A meta-analysis. *Biogeosciences* **12**, 1671–1682 (2015).
7. U. Riebesell, I. Zondervan, B. Rost, P. D. Tortell, R. E. Zeebe, F. M. M. Morel, Reduced calcification of marine plankton in response to increased atmospheric CO_2. *Nature* **407**, 364–367 (2000).
8. K. T. Lohbeck, U. Riebesell, T. B. H. Reusch, Adaptive evolution of a key phytoplankton species to ocean acidification. *Nat. Geosci.* **5**, 346–351 (2012).
9. L. Schlüter, K. T. Lohbeck, M. A. Gutowska, J. P. Gröger, U. Riebesell, T. B. H. Reusch, Adaptation of a globally important coccolithophore to ocean warming and acidification. *Nat. Clim. Change* **4**, 1024–1030 (2014).
10. M. M. Desai, D. S. Fisher, A. W. Murray, The speed of evolution and maintenance of variation in asexual populations. *Curr. Biol.* **17**, 385–394 (2007).
11. G. I. Lang, D. P. Rice, M. J. Hickman, E. Sodergren, G. M. Weinstock, D. Botstein, M. M. Desai, Pervasive genetic hitchhiking and clonal interference in forty evolving yeast populations. *Nature* **500**, 571–574 (2013).
12. S. F. Elena, V. S. Cooper, R. E. Lenski, Punctuated evolution caused by selection of rare beneficial mutations. *Science* **272**, 1802–1804 (1996).
13. Z. D. Blount, C. Z. Borland, R. E. Lenski, Historical contingency and the evolution of a key innovation in an experimental population of *Escherichia coli*. *Proc. Natl. Acad. Sci. U.S.A.* **105**, 7899–7906 (2008).
14. A. J. Irwin, Z. V. Finkel, F. E. Müller-Karger, L. Troccoli Ghinaglia, Phytoplankton adapt to changing ocean environments. *Proc. Natl. Acad. Sci. U.S.A.* **112**, 5762–5766 (2015).
15. IPCC, *Climate Change 2013: The Physical Science Basis, Contribution of Working Group I to the Fifth Assessment Report of the Intergovernmental Panel on Climate Change*, T. F. Stocker, D. Qin, G.-K. Plattner, M. M. B. Tignor, S. K. Allen, J. Boschung, A. Nauels, Y. Xia, V. Bex, P. M. Midgley, Eds. (Cambridge University Press, Cambridge, 2013), p. 1535.
16. F. Melzner, J. Thomsen, W. Koeve, A. Oschlies, M. A. Gutowska, H. W. Bange, H. Peter Hansen, A. Körtzinger, Future ocean acidification will be amplified by hypoxia in coastal habitats. *Mar. Biol.* **160**, 1875–1888 (2013).
17. S. Collins, Many possible worlds: Expanding the ecological scenarios in experimental evolution. *Evol. Biol.* **38**, 3–14 (2011).
18. R. E. Lenski, M. R. Rose, S. C. Simpson, S. C. Tadler, Long-term experimental evolution in *Escherichia coli*. I. Adaptation and divergence during 2,000 generations. *Am. Nat.* **138**, 1315–1341 (1991).
19. L. Schlüter, Long-term adaptation of the coccolithophore *Emiliania huxleyi* to ocean acidification and global warming, thesis, University of Kiel, Kiel, Germany (2016).
20. S. F. Elena, R. E. Lenski, Evolution experiments with microorganisms: The dynamics and genetic bases of adaptation. *Nat. Rev. Genet.* **4**, 457–469 (2003).
21. P. Westbroek, J. R. Young, K. Linschooten, Coccolith production (biomineralization) in the marine alga *Emiliania huxleyi*. *J. Eukaryotic Microbiol.* **36**, 368–373 (1989).
22. P. J. Gerrish, R. E. Lenski, The fate of competing beneficial mutations in an asexual population. *Genetica* **102–103**, 127–144 (1998).
23. E. P. Y. Tang, The allometry of algal growth rates. *J. Plankton Res.* **17**, 1325–1335 (1995).
24. S. D. Rokitta, U. John, B. Rost, Ocean acidification affects redox-balance and ion-homeostasis in the life-cycle stages of *Emiliania huxleyi*. *PLOS One* **7**, e52212 (2012).
25. S. F. Elena, R. E. Lenski, Epistasis between new mutations and genetic background and a test of genetic canalization. *Evolution* **55**, 1746–1752 (2001).
26. G. Langer, G. Nehrke, I. Probert, J. Ly, P. Ziveri, Strain-specific responses of *Emiliania huxleyi* to changing seawater carbonate chemistry. *Biogeosciences* **6**, 2637–2646 (2009).
27. J. A. Raven, K. Crawfurd, Environmental controls on coccolithophore calcification. *Mar. Ecol. Prog. Ser.* **470**, 137–166 (2012).
28. L. Mackinder, G. Wheeler, D. Schroeder, U. Riebesell, C. Brownlee, Molecular mechanisms underlying calcification in coccolithophores. *Geomicrobiol. J.* **27**, 585–595 (2010).
29. S. M. Scheiner, Genetics and evolution of phenotypic plasticity. *Annu. Rev. Ecol. Syst.* **24**, 35–68 (1993).
30. E. Schaum, B. Rost, A. J. Millar, S. Collins, Variation in plastic responses to ocean acidification in a globally distributed picoplankton species. *Nat. Clim. Change* **3**, 298–302 (2013).
31. S. Sett, L. T. Bach, K. G. Schulz, S. Koch-Klavsen, M. Lebrato, U. Riebesell, Temperature modulates coccolithophorid sensitivity of growth, photosynthesis and calcification to increasing seawater pCO_2. *PLOS One* **9**, e88308 (2014).
32. T. B. H. Reusch, Climate change in the oceans: Evolutionary versus phenotypically plastic responses in marine animals and plants. *Evol. Appl.* **7**, 104–122 (2014).
33. C. K. Ghalambor, J. K. McKay, S. P. Carroll, D. N. Reznick, Adaptive versus non-adaptive phenotypic plasticity and the potential for contemporary adaptation in new environments. *Funct Ecol.* **21**, 394–407 (2007).
34. S. Collins, G. Bell, Phenotypic consequences of 1,000 generations of selection at elevated CO_2 in a green alga. *Nature* **431**, 566–569 (2004).
35. L. Mackinder, G. Wheeler, D. Schroeder, P. von Dassow, U. Riebesell, C. Brownlee, Expression of biomineralization-related ion transport genes in *Emiliania huxleyi*. *Environ. Microbiol.* **13**, 3250–3265 (2011).
36. K. Suffrian, K. G. Schulz, M. Gutowska, U. Riebesell, M. Bleich, Cellular pH measurements in *Emiliania huxleyi* reveal pronounced membrane proton permeability. *New Phytol.* **190**, 595–608 (2011).
37. K. T. Lohbeck, U. Riebesell, T. B. H. Reusch, Gene expression changes in the coccolithophore *Emiliania huxleyi* after 500 generations of selection to ocean acidification. *Proc. Biol. Sci.* **281**, 20140003 (2014).

38. C. Hamm, V. Smetacek, Armor: Why, when, and how, in *Evolution of Primary Producers in the Sea,* P. Falkowski, A. H. Knoll, Eds. (Academic Press, Burlington, MA, 2011), pp. 311–332.
39. T. B. H. Reusch, P. W. Boyd, Experimental evolution meets marine phytoplankton. *Evolution* **67**, 1849–1859 (2013).
40. S. M. Kidwell, Biology in the Anthropocene: Challenges and insights from young fossil records. *Proc. Natl. Acad. Sci. U.S.A.* **112**, 4922–4929 (2015).
41. M. H. Pespeni, E. Sanford, B. Gaylord, T. M. Hill, J. D. Hosfelt, H. K. Jaris, M. LaVigne, E. A. Lenz, A. D. Russell, M. K. Young, S. R. Palumbi, Evolutionary change during experimental ocean acidification. *Proc. Natl. Acad. Sci. U.S.A.* **110**, 6937–6942 (2013).
42. J. M. Sunday, R. N. Crim, C. D. G. Harley, M. W. Hart, Quantifying rates of evolutionary adaptation in response to ocean acidification. *PLOS One* **6**, e22881 (2011).
43. J. M. Sunday, P. Calosi, S. Dupont, P. L. Munday, J. H. Stillman, T. B. H. Reusch, Evolution in an acidifying ocean. *Trends Ecol. Evol.* **29**, 117–125 (2014).
44. C.-E. Schaum, B. Rost, S. Collins, Environmental stability affects phenotypic evolution in a globally distributed marine picoplankton. *ISME J.* **10**, 75–84 (2015).
45. S. Collins, B. Rost, T. A. Rynearson, Evolutionary potential of marine phytoplankton under ocean acidification. *Evol. Appl.* **7**, 140–155 (2014).
46. D. R. Kester, I. W. Duedall, D. N. Connors, R. M. Pytkowicz, Preparation of artificial seawater. *Limnol. Oceanogr.* **12**, 176–179 (1967).
47. E. Lewis, D. W. R. Wallace, *Program Developed for CO_2 System Calculations* (Oak Ridge National Laboratory, U.S. Department of Energy, Oak Ridge, TN, 1998).

Acknowledgments: We thank R. Ebbinghaus, K. Beining, J. Meyer, G. Faucher, S. Audritz, D. Gill, A. Ludwig, and K. Nachtigall for laboratory assistance and M. Gutowska for advice. **Funding:** This project was funded through the Cluster of Excellence "The Future Ocean" and the Bundesministerium für Bildung und Forschung (BMBF) project "Biological Impacts of Ocean Acidification" (BIOACID). **Author contributions:** L.S. and T.B.H.R. conceived the study; K.T.L. and L.S. performed the experiments; K.T.L., T.B.H.R., and L.S. analyzed the data; J.P.G. conducted the time series analyses; L.S. and T.B.H.R. wrote the manuscript; and all authors discussed and edited the manuscript. **Competing interests:** The authors declare that they have no competing interests. **Data and materials availability:** All data needed to evaluate the conclusions in the paper are present in the paper and/or the Supplementary Materials. Additional data related to this paper may be requested from the authors. Raw data were deposited in the World Data Center for Marine Environmental Sciences (WDC-MARE) (accession http://doi.pangaea.de/10.1594/PANGAEA.846062).

Submitted 17 November 2015
Accepted 15 June 2016
Published 8 July 2016
10.1126/sciadv.1501660

Citation: L. Schlüter, K. T. Lohbeck, J. P. Gröger, U. Riebesell, T. B. H. Reusch, Long-term dynamics of adaptive evolution in a globally important phytoplankton species to ocean acidification. *Sci. Adv.* **2**, e1501660 (2016).

ScienceAdvances
AAAS

Long-term dynamics of adaptive evolution in a globally important phytoplankton species to ocean acidification

Lothar Schlüter, Kai T. Lohbeck, Joachim P. Gröger, Ulf Riebesell and Thorsten B. H. Reusch (July 8, 2016)

Sci Adv 2016, 2:.
doi: 10.1126/sciadv.1501660